

Analysis of the Data from Compton X-ray Polarimeters which Measure the Azimuthal and Polar Scattering Angles

H. Krawczynski^a

^a*Washington University in St. Louis, Department of Physics and the McDonnell Center
for the Space Sciences, 1 Brookings Dr., CB 1105, St Louis, MO 63130*

Abstract

X-ray polarimetry has the potential to make key-contributions to our understanding of galactic compact objects like binary black hole systems and neutron stars, and extragalactic objects like active galactic nuclei, blazars, and Gamma Ray Bursts. Furthermore, several particle astrophysics topics can be addressed including uniquely sensitive tests of Lorentz invariance. In the energy range from 10 keV to several MeV, Compton polarimeters achieve the best performance. In this paper we evaluate the benefit that comes from using the azimuthal and polar angles of the Compton scattered photons in the analysis, rather than using the azimuthal scattering angles alone. We study the case of an ideal Compton polarimeter and show that a Maximum Likelihood analysis which uses the two scattering angles lowers the Minimum Detectable Polarization (MDP) by $\approx 20\%$ compared to a standard analysis based on the azimuthal scattering angles alone. The accuracies with which the polarization fraction and the polarization direction can be measured improve by a similar amount. We conclude by discussing potential applications of Maximum Likelihood analysis methods for various polarimeter experiments.

Keywords: Hard X-ray Polarimetry, Instrumentation, Compton Effect, X-ray detectors, Analysis Techniques, Maximum Likelihood Analysis

Email address: krawcz@wuphys.wustl.edu, Tel. 314 935 8553, Fax. 314 935 6219 (H. Krawczynski)

1. Introduction

Some of the most interesting astrophysical objects are too small to be spatially resolved by present-day telescopes: the Schwarzschild radius of a galactic stellar mass black hole of $M_1 = 10 M_\odot$ solar masses at a distance of d_3 kpc corresponds to an angular extent of $2 \times 10^{-4} M_1/d_3 \mu\text{arcsec}$; for an extragalactic supermassive black hole of $M_9 = 10^9 M_\odot$ solar masses at a distance of $20 d_6$ Mpc, the Schwarzschild radius corresponds to an angular extent of $M_9/d_6 \mu\text{arcsec}$; a time of $\Delta t = 1000$ sec (in the observer frame) after the explosion of a Gamma Ray Bursts (GRB) at redshift $z = 1$, a GRB jet has an angular extent of $1.2 \times 10^{-10} (\Gamma/10^3)^2 (\Delta t/1000 \text{ sec}) (\sin(\theta)/\sin(1^\circ)) \mu\text{arcsec}$ if we assume (somewhat unrealistically) a constant jet expansion velocity with a bulk Lorentz factor Γ along an angle θ to the line of sight. The numbers demonstrate the difficulties to image these objects. In the absence of imaging information, X-ray spectropolarimetric observations can deliver the additional information required to decide between models which cannot be distinguished based on spectroscopic data alone [1, 2, 3, 4, 5, 6, 7, 8, 9]. An X-ray polarimeter can deliver for each time interval not only an energy spectrum of the X-ray flux $F(E)$, but also the energy spectra of the X-ray polarization degree $a_0(E)$ and the X-ray polarization direction $\phi_0(E)$. X-ray polarimetry will make a big leap when NASA will launch the Gravity and Extreme Magnetism SMEX (*GEMS*) mission in 2014 [10]. *GEMS* will use two Wolter type mirror assemblies to focus 2-10 keV X-rays onto two photoeffect polarimeters. Each polarimeter is made of a photoelectron-tracking time projection chamber. A student experiment will give additional polarization sensitivity at 0.5 keV.

In this paper, we discuss the analysis of data from polarimeters in the > 10 keV to several MeV energy range based on the detection of Compton-scattered photons. Compton polarimeters use the fact that photons scatter preferentially perpendicular to the orientation of the electric field vector of a polarized X-ray beam. Several past and present satellites were equipped with detector configurations which – although not designed for Compton polarimetry – were used to constrain the polarization of the X-ray emission from cosmic sources based on the analysis of Compton events (see [6, 8] and references therein). Recently, two experiments on board of the *INTEGRAL* (International Gamma-Ray Astrophysics Laboratory) satellite were used to measure the polarization of the 100 keV to 1 MeV emission from the Crab Pulsar and the Crab Nebula. Events scattered between different Ge detectors

of the *SPI* (SPectrometer on *INTEGRAL*) detector were used to measure a polarization degree of $46\% \pm 10\%$ and a polarization direction aligned with the orientation of the X-ray jet [11]. The analysis of events scattered between different CdTe detectors of the *IBIS* (Imager on-Board *INTEGRAL* Satellite) detector confirmed the large polarization fraction of the hard X-rays [12]. In a similar fashion, Compton polarimetry was used with the Ge detectors onboard of the RHESSI experiment to constrain the polarization of solar flares in the >200 keV energy range [13, 14]. A report of polarized γ -ray emission from a Gamma-Ray Bursts remained controversial after several independent analyses did not confirm the result [15, 16, 17]. The soft gamma-ray telescope on board of the Japanese/US ASTRO-H mission (launch foreseen in 2013) will be able to measure the polarization of hard X-rays by detecting Compton scattered photons with a combination of Si pad detectors and Cadmium Telluride (CdTe) pixel detectors [18].

A considerable number of dedicated Compton X-ray polarimeters have been described in the literature, see for example [19, 6, 20, 21, 23, 24, 22, 8, 25] and references therein. Whereas some polarimeters are designed to measure exclusively the azimuthal scattering angles (e.g. [20, 23]), other experiments also give information about the polar scattering angle on event to event basis (e.g. [18, 21, 22]). The analyses used so far for both types of experiments are based on fitting a constant offset plus a sine curve to the azimuthal scattering angle distributions. In this paper, we explore for the first time the sensitivity gain that can be achieved when using both, the azimuthal and the polar scattering angles in the analysis with the help of a Maximum Likelihood analysis method. In Sects. 2 and 3 we motivate the use of the polar and the azimuthal scattering angles based on the properties of the Klein-Nishina cross section and describe the standard analysis method and the Maximum Likelihood analysis method. In Sect. 4 we discuss simulations of an ideal Compton polarimeter and evaluate the sensitivity gain achieved with the Maximum Likelihood analysis method. In Sect. 5 we summarize the results.

2. Compton Scatterings: Basics

Compton scatterings are governed by Compton's formula and by the Klein-Nishina cross section. Compton's formula reads:

$$\Delta\lambda = \frac{h}{m_e c} (1 - \cos\theta) \quad (1)$$

where h is Planck's constant, m_e is the electron mass, c is the speed of light, and θ the polar scattering angle. The Klein-Nishina cross section is given by (see e.g. [26]):

$$\frac{d\sigma}{d\Omega} = \frac{r_0^2}{2} \frac{k_1^2}{k_0^2} \left[\frac{k_0}{k_1} + \frac{k_1}{k_0} - 2\sin^2\theta\cos^2\eta \right] \quad (2)$$

with r_0 the classical electron radius, \mathbf{k}_0 and \mathbf{k}_1 the wave-vectors before and after scattering, θ the scattering angle (the angle between \mathbf{k}_0 and \mathbf{k}_1), and η the azimuthal scattering angle, i.e. the angle between the electric vector of the incident photon and the scattering plane. Averaging over the azimuthal scattering angles gives the cross section for a scattering of a polarized photon with a polar scattering angle θ irrespective of η :

$$\frac{d\sigma}{d\Omega}(\theta) = \frac{1}{2} \left(\frac{d\sigma}{d\Omega} \right)_{\eta=0} + \frac{1}{2} \left(\frac{d\sigma}{d\Omega} \right)_{\eta=\pi/2} = \frac{r_0^2}{2} \frac{k_1^2}{k_0^2} \left[\frac{k_0}{k_1} + \frac{k_1}{k_0} - \sin^2\theta \right] \quad (3)$$

This cross section equals the Klein-Nishina cross section for unpolarized incident photons.

As linearly polarized X-rays are preferentially scattered perpendicular to the orientation of the electric field vector, the probability density function of the azimuthal scattering angle η exhibits a modulation of the form:

$$P(\eta) = \frac{1}{\pi} \left(1 + b \cos \left[2 \left(\eta - \frac{\pi}{2} \right) \right] \right) \quad (4)$$

The modulation amplitude b of the azimuthal scattering angle distribution can be computed from the Klein-Nishina cross section:

$$b(\theta) = \frac{\left(\frac{d\sigma}{d\Omega} \right)_{\eta=\pi/2} - \left(\frac{d\sigma}{d\Omega} \right)_{\eta=0}}{\left(\frac{d\sigma}{d\Omega} \right)_{\eta=\pi/2} + \left(\frac{d\sigma}{d\Omega} \right)_{\eta=0}} = \frac{\sin^2\theta}{k_0/k_1 + k_1/k_0 - \sin^2\theta} \quad (5)$$

Fig. 1 shows the modulation amplitude as function of θ for several initial photon energies. The panel shows that events with scattering angles close to $\pi/2$ exhibit a larger modulation amplitude. As a consequence, those events have a higher information content than events with scattering angles close to 0 and close to π .

3. Analysis Methods

In the standard analysis the azimuthal scattering angles ϕ are histogrammed. The polarization is determined by fitting the model

$$n(a_0, \phi_0; \phi) = \bar{n} (1 + a_0 \mu \cos[2(\phi - \phi_0)]) \quad (6)$$

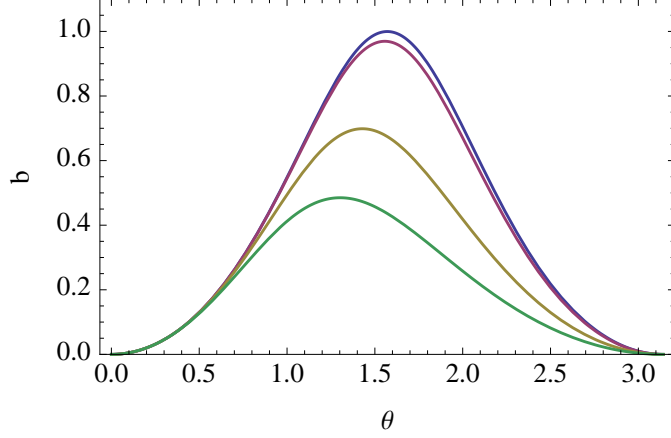


Figure 1: The modulation amplitude b of the azimuthal scattering angle from Compton scatterings as function of the polar scattering angle for photon energies of 10 keV, 100 keV, 500 keV, and 1 MeV (from top to bottom).

with a χ^2 -fit to the histogram. The value \bar{n} is the mean number of entries in each bin of the histogram: $\bar{n} = n_0/N$, if n_0 events were recorded and the histogram has N bins. The fitting parameter a_0 is the fractional polarization of the beam and equals 1 for a 100% polarized beam and 0 for an unpolarized beam. The parameter μ is the “modulation factor” which gives the modulation amplitude for a 100% polarized beam. In general, μ depends on the physics of Compton scatterings and on the design of the polarimeter. In the following we will consider an “ideal polarimeter” which detects all Compton scattered photons and gives the scattering angles with very high precision. In this particular case, μ is simply the modulation amplitude b averaged over all solid angles and the Klein-Nishina cross section. For primary photon energies of 10 keV, 100 keV, and 1 MeV the averaged modulation factor equals 0.5, 0.48, and 0.25, respectively. The angle ϕ_0 is the fitted polarization direction (in the coordinates of the polarimeter).

If a_T and ϕ_T are the true polarization fraction and polarization direction, the probability distribution of the measured values a_0 and ϕ_0 is given by [27, 28, 7]:

$$P(a_0, \phi_0) = \frac{N \bar{n}^2 a_0 \mu^2}{4\pi\sigma^2} \exp \left[-\frac{N \bar{n}^2 \mu^2}{4\sigma^2} (a_0^2 + a_T^2 - 2a_0 a_T \cos(\phi_0 - \phi_T)) \right] \quad (7)$$

In the absence of background, the statistical error on the number of counts per bin is given by Poisson statistics: $\sigma = \sqrt{\bar{n}}$. Integration of this distribution over ϕ_0 gives the probability to measure a polarization degree a_0 independent of ϕ_0 :

$$P(a_0) = \frac{N \bar{n}^2 a_0 \mu^2}{2\sigma^2} \exp \left[-\frac{N \bar{n}^2 \mu^2}{4\sigma^2} (a_0^2 + a_T^2) \right] I_0 \left(\frac{N \bar{n}^2 \mu^2 a_0 a_T}{2\sigma^2} \right) \quad (8)$$

with I_0 the modified Bessel function of order zero. This probability distribution can be used to determine the minimum fractional polarization which can be measured at a certain confidence level. The Minimum Detectable Polarization (MDP) is defined as the fractional polarization $a_{1\%}$ which will be measured in the absence of any true polarization $a_T = 0$ with a chance probability of 1%:

$$P(a > a_{1\%}) = \int_{a_{1\%}}^{\infty} P(a_0) da_0 = 1\% \quad (9)$$

Integration gives for $\sigma = \sqrt{\bar{n}}$:

$$MDP \approx \frac{4.29}{\mu \sqrt{n_0}} \quad (10)$$

As an alternative to the standard method, we evaluate below a Maximum Likelihood analysis. The method uses an event list as input:

$$\mathcal{L} = \{(E_i, \theta_i, \phi_i), i = 1 \dots n_0\} \quad (11)$$

with E_i , θ_i , and ϕ_i being the energy, polar scattering angle, and azimuthal scattering angle of the i^{th} event, assumed here to be measured with high precision. The polarization degree a_0 and polarization direction ϕ_0 are determined by maximizing the Likelihood function:

$$\lambda(a_0, \phi_0) = \prod_{i=0}^{n_0} P(\phi_i; a_0, \phi_0, E_i, \theta_i) \quad (12)$$

In practice, it is more convenient to maximize the logarithm of the likelihood function $\ln \lambda$ than to maximize λ . The probability of measuring the azimuthal scattering angle ϕ_i given the a_0 , ϕ_0 , E_i , and θ_i is given by the expression:

$$P(\phi_i; a_0, \phi_0, E_i, \theta_i) = \frac{1}{\pi} (1 + a_0 \mu(E_i, \theta_i) \cos[2(\phi_i - \phi_0)]) \quad (13)$$

with $\mu(E_i, \theta_i)$ being the modulation factor for the incident photon energy E_i and the polar scattering angle θ_i . For the ideal polarimeter, μ is given by Equ. (5). The maximization of $\ln \lambda$ gives the maximum likelihood estimates $a_{0,\text{ML}}$ and $\phi_{0,\text{ML}}$ of the polarization fraction and polarization direction, respectively.

We recommend to calculate the statistical significance of the detection of a polarized signal by simulating the background and the signal assuming the null hypothesis (an unpolarized signal) and calculating the fraction of simulated event lists with best-fit polarization degrees exceeding the observed one.

One can estimate the uncertainty on the fit-parameters by mapping the Bayesian posterior probability density function [29] (see also [30]):

$$p(a_0, \phi_0) = \frac{\lambda(a_0, \phi_0)}{\int_0^1 da'_0 \int_0^\pi d\phi'_0 \lambda(a'_0, \phi'_0)} \quad (14)$$

The function p can be used to plot a region $\mathcal{R}_\alpha(\beta)$ (or several regions) which contains the true value a_T and ϕ_T with a certain probability α :

$$\mathcal{R}_\alpha(\beta) = \{(a_0, \phi_0) \mid p(a_0, \phi_0) > \beta, a_0 \in [0, 1], \phi_0 \in [0, \pi]\} \quad (15)$$

with β is chosen such that

$$\int_{\mathcal{R}_\alpha(\beta)} da'_0 d\phi'_0 p(a'_0, \phi'_0) = \alpha \quad (16)$$

4. Achieved Performance

We evaluated the performance of the standard analysis and the Maximum Likelihood analysis by generating simulated data sets for $a_T = 0$ and the n_0 -values given in Table 1. For each parameter configuration, 10,000 data sets were simulated. We limited the study to primary photon energies of 100 keV. Individual events were generated by first drawing a polar scattering angle from the distribution given by Equ. (3). Subsequently, an azimuthal scattering angle was generated according to the distribution given by Equ. (4). The event lists were analyzed with the two analysis methods described above.

Figure 2 shows the distributions of the best-fit polarization fraction a_0 for the case of no polarization $a_T = 0$ for data sets with $n_0 = 10,000$ events. The

n_0	MDP Equ. (10) [%]	MDP Method [%]	Stand. Method [%]	MDP Max. Lik. Method [%]
1000	28.3	28.3		23.8
3000	16.3	16.2		13.7
10000	8.9	9.0		7.4
50000	4.0	3.9		3.3

Table 1: Summary of simulation of data sets for a primary photon energy of 100 keV. For each number of Compton events, 10,000 data sets were simulated assuming no inherent polarization $a_T = 0$. For each data set the polarization fraction a_0 was reconstructed with various methods. The a_0 -distributions were used to determine the Minimum Detectable Polarization (MDP) being the value that is larger than 99% of the reconstructed MDP values.

Maximum Likelihood method gives on average smaller best-fit polarization values. The MDP is calculated by determining the a_0 -value which is larger than 99% of all fitted values. For $n_0 = 10,000$ the standard method and the Maximum Likelihood method give MDPs of 0.089 and 0.074, respectively. Thus, the Maximum Likelihood method results in a reduction of the MDP by 21%. It should be noted that the observed MDP for the standard method agrees well with the estimate from Equ. (10).

Figure 3 shows the MDPs achieved with the two methods for n_0 -values ranging from 1000 to 50,000 for the Maximum Likelihood method, the standard method, and a simpler method. In the case of the “simple method” the polarization degree is derived from the maximum number n_{\max} and minimum number n_{\min} of entries in the azimuthal scattering angle histogram according to

$$a_0 = \frac{1}{\mu} \frac{n_{\max} - n_{\min}}{n_{\max} + n_{\min}}. \quad (17)$$

Whereas the standard method uses the contents of all bins in the histogram to estimate a_0 , the simple method uses only the contents of two bins (the bins with the minimum and maximum number of counts). It is thus expected that standard method gives more precise estimates of a_0 . In the absence of a true polarization signal, the standard method should thus give on average smaller a_0 -values than the simple method. As a result, the standard method leads to a smaller a_0 -value that can be detected at a certain confidence level than the simple method. Figure 3 indeed shows that the simple method performs markedly poorer than the standard method. Whereas the MDP achieved with the standard method is independent of the number of bins

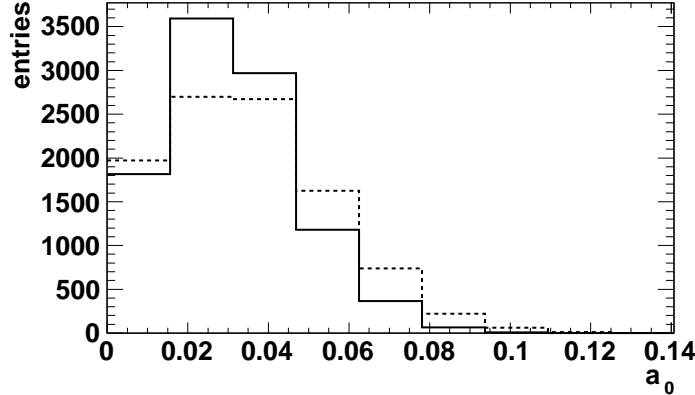


Figure 2: Distribution of the reconstructed polarization fraction a_0 for a true polarization fraction of $a_T = 0$. The solid lines show the results for the Maximum Likelihood analysis which uses the polar and azimuthal scattering angles of the Compton events; the dashed lines show the results for the standard analysis which uses only the azimuthal scattering angles ($n_0 = 10,000$).

used in the azimuthal scattering histogram (as long as the number of bins is not too small to smear out the modulation, and not too large to reduce the number of entries per bin to values below 10), the simple method performs poorer the more bins are used in this histogram.

Compared to the simple method and the standard method, the Maximum Likelihood leads to a reduction of the MDP by 255% and 21%, respectively, independent of n_0 . As mentioned before, the improvement relative to the simple method depends on the number of bins used in the azimuthal scattering angle histogram. Figure 4 shows the distributions of the fitted a_0 and ϕ_0 -values for $a_T = 0.25$, $\phi_T = \pi/2$, and $n_0 = 10,000$. The standard analysis and the Maximum Likelihood analysis give 68% confidence intervals on a_0 of 29% and 24%, respectively. For the polarization angle ϕ_0 the 68% confidence intervals are 0.06 rad (3.4°) and 0.048 rad (2.7°) for the two respective methods.

5. Summary and Discussion

Photons of a linearly polarized X-ray beam Compton scatter preferentially into the direction perpendicular to the preferred orientation of the electric

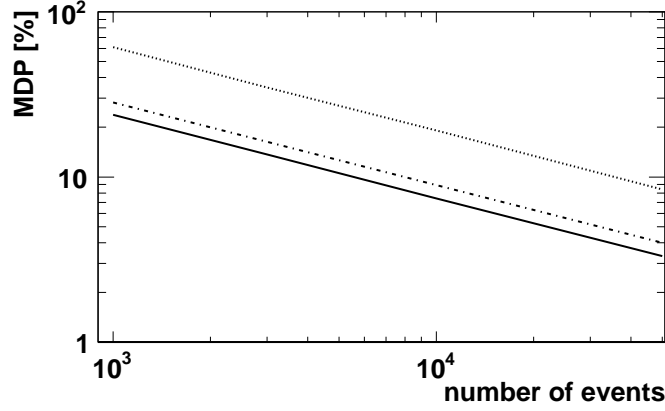


Figure 3: Minimum Detectable Polarization (MDP) as function of the number of Compton events for (from below to above) the Maximum Likelihood method (solid line), the standard method (dashed line), and for a simpler method (dotted line) in which the polarization degree is derived from the maximum and minimum number of entries in the azimuthal scattering angle histogram. The Maximum Likelihood method leads to an improvement by 21% compared to the standard method.

field vector. The modulation of the azimuthal scattering angle distribution depends on the polar scattering angle θ . The modulation is most pronounced for photons with polar scattering angles close to $\pi/2$ (slightly less for higher energies), and weakest for forward-scattered and back-scattered photons. In this paper, we have described a Maximum Likelihood analysis which uses the polar and azimuthal scattering angles of all detected Compton events to estimate the polarization degree and the polarization direction. For an ideal Compton polarimeter, the Maximum Likelihood analysis results in a reduction of the MDP by 21%. The accuracies ($\sigma_{68\%}$ -values) with which non-zero polarization degrees and polarization directions can be measured are reduced by similar fractional amounts. Note that the improvement by 21% results from the properties of Compton scatterings. The improvement is somewhat modest, but is consistent with expectations based on Eqs. (5) and (10): for events with a certain modulation factor μ the MDP scales inversely proportional to μ (Equ. 10). For the “best events” the modulation factor is close to 1; for energies $\ll m_e c^2$ the average modulation factor is 0.5. The decrease of the MDP should thus have a value of between 1 and $1/\mu = 2$.

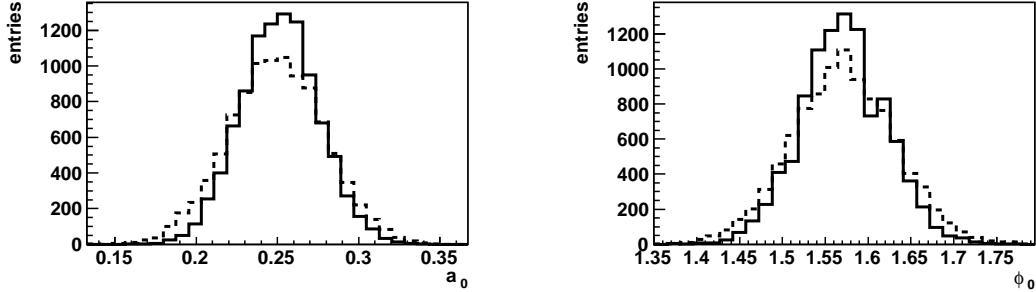


Figure 4: Distribution of the reconstructed polarization fraction a_0 (left panel) and the reconstructed polarization degree ϕ_0 (right panel) for a true polarization fraction of $a_T = 0.25$ and a true polarization direction $\phi_T = \pi/2$. The solid lines show the results for the Maximum Likelihood analysis which uses the polar and azimuthal scattering angles of the Compton events; the dashed lines show the results for the standard analysis which uses only the azimuthal scattering angles (both panels are for $n_0 = 10,000$).

For a real-world Compton polarimeter, a Maximum Likelihood analysis could be performed with the Likelihood function given by Eqs. (12) and (13). For experiments with non-uniform acceptance (e.g. for the ASTRO-H soft gamma-ray telescope of the ASTRO-H mission), the PDF of Equ. (13) should be replaced with a PDF obtained from Monte Carlo simulations. The PDF could then depend on a variety of measured parameters, e.g. the estimated energy of the primary event, the location of the first interaction, and the polar and azimuthal scattering angles.

A Maximum Likelihood approach could also be used for the analysis of the data from photo-effect polarimeters as the gas polarimeters described in [31, 32, 33, 34, 35, 36]. The approach can be implemented by determining the modulation factor as a function of a set \mathcal{O}_i of suitable observables for each event, and by using the modulation factor $\mu(\mathcal{O}_i)$ in Equ. (13). One obvious choice is to use the reconstructed energy of the events: $\mathcal{O}_i = \{E_i\}$. Soffitta et al. [32] and Depaola & Longo [33] discuss the pronounced energy dependence of the modulation factor. Some of the energy dependence stems from the atomic physics of the photon-absorption, i.e. the modulation factor for s electrons is larger than for p and d electrons and Auger electrons are emitted isotropically. Some of the energy dependence stems from the detection technique as the properties of the recorded photoelectron tracks depend on the

photon energy. One may use additional properties of an event which have an impact on the effective modulation factor, e.g., the track length or the number of triggered pixels, the ellipticity of the track image when analyzed with a second moment analysis, or the estimated error on the reconstructed azimuthal scattering angle. The usage of $\mu(\mathcal{O}_i)$ in Equ. (13) will improve the sensitivity of the polarimeter as the individual events are weighted according to their information content.

Acknowledgements: HK acknowledges NASA for support from the APRA program under the grant NNX10AJ56G and support from the high-energy physics division of the DOE. HK thanks Martin Israel and an anonymous referee for helpful comments. HK is grateful for support by the Washington University McDonnell Center for the Space Sciences.

References

- [1] Rees, M. J. 1975, MNRAS, 179, 691
- [2] Lightman, A. P., Shapiro, S. L. 1975, ApJ, 198, 73
- [3] Lightman, A. P., Shapiro, S. L. 1976, ApJ, 203, 701
- [4] Meszaros, P., Novick, R., Szentgyorgyi, A., Chanan, G. A., Weisskopf, M. C. 1988, ApJ, 324, 1056
- [5] Rees, M. J., Meszaros, P. 1994, ApJ, 430, L93
- [6] Lei, F., Dean, A. J., Hills, G. L. 1997, Space Sci. Rev., 82, 309
- [7] Weisskopf, M. C., Elsner, R. F., Hanna, D., Kaspi, V. M., O’Dell, S. L., Pavlov, G. G., Ramsey, B. D. 2006, “The prospects for X-ray polarimetry and its potential use for understanding neutron stars”, paper presented at the 363rd Heraeus Seminar in Bad Honef, Germany, [astro-ph/0611483]
- [8] Bellazini, R., Costa, E., Matt, G., Tagliaferri, G. (eds.), “X-ray Polarimetry: A New Window in Astrophysics”, Cambridge Contemporary Astrophysics (2010)
- [9] H. Krawczynski, A. Garson III, Q. Guo et al. 2011, Astropart. Phys., 34, 550

- [10] Swank, J., et al. <http://heasarc.gsfc.nasa.gov/docs/gems/>
- [11] Dean, A. J., Clark, D. J., Stephen, J. B., et al. 2008, *Science*, 321, 1183
- [12] Forot, M., Laurent, P., Grenier, I. A., Gouiffès, C., Lebrun, F. 2008, *ApJL*, L688, 29
- [13] Boggs, S. E., Coburn, W., Kalemci, E. 2006, *ApJ*, 638, 1129
- [14] Suarez-Garcia, E., Hajdas, W., Wigger, C., Arzner, K., Güdel, M., Zehnder, A., & Grigis, P. 2006, *Sol. Phys.*, 239, 149
- [15] Coburn, W., Boggs, S. E. 2003, *Nature*, 423, 415
- [16] Rutledge, R. E., Fox, D. B. 2004, *MNRAS*, 350, 1288
- [17] Wigger, C., Hajdas, W., Arzner, K., Güdel, M., & Zehnder, A. 2004, *ApJ*, 613, 1088
- [18] Takahashi, T., Kelley, R., Mitsuda, K., et al., “The NeXT Mission”, *Space Telescopes and Instrumentation 2008: Ultraviolet to Gamma Ray*. Edited by Turner, Martin J. L.; Flanagan, Kathryn A. *Proceedings of the SPIE*, Volume 7011, pp. 70110O-70110O-14, 2008.
- [19] Costa, E., Cinti, M. N., Feroci, M., Matt, G., Rapisarda, M. 1995, *NIMA*, 366, 161
- [20] Mizuno, T., Kamae, T., Ng, J., et al. 2005, *NIMA*, 540, 158
- [21] Krawczynski, H., Garson, A. III, Martin, J., et al. 2009, *IEEE Transactions of Nuclear Science*, 56, 3607
- [22] Greiner, J., et al. 2009, *Experimental Astronomy*, 23, 91
- [23] McConnell, M. L., Angelini, L., Baring, M. G., et al. 2009a, *AIP Conf. Proc.*, 1133, 64
- [24] McConnell, M. L., Bancroft, C., Bloser, P. F., Connor, T., Legere, J., Ryan, J. M. 2009b, *SPIE*, 7435, 13
- [25] Vadawale, S. V., Paul, B., Pendharkar, J., & Naik, S. 2010, *NIMA*, 618, 182

- [26] Evans, R. D. 1955, “The atomic nucleus”, New York: McGraw-Hill
- [27] Vinokur, M. 1965, *Annales d’Astrophysique*, 28, 412
- [28] Jenkins, G. M., Watts, D. G. 1968, “Spectral Analysis and Its Applications” (Holden-Day, San Francisco)
- [29] Nakamura, K., et al. (Particle Data Group) 2010, *J. Phys. G* 37, 075021, Chapter 33
- [30] Weisskopf, M. C., Elsner, R. F., & O’Dell, S. L. 2010, *Proc. Spie*, 7732, 11 [arXiv:1006.3711]
- [31] Costa, E., Soffitta, P., Bellazzini, R., Brez, A., Lumb, N., & Spandre, G. 2001, *Nature*, 411, 662
- [32] Soffitta, P., et al. 2001, *NIMA*, 469, 164
- [33] Depaola, G. O., & Longo, F. 2006, *NIMA*, 566, 590
- [34] Muleri, F., et al. 2008, *NIMA*, 584, 149
- [35] Muleri, F., et al. 2010, *NIMA*, 620, 285
- [36] Black, J. K., et al. 2010, *Proc. Spie*, 7732